NeuroImage: Clinical 17 (2018) 976–986

Contents lists available at ScienceDirect

NeuroImage: Clinical

journal homepage: www.elsevier.com/locate/ynicl

Visual processing deficits in 22q11.2 Deletion Syndrome

Marjan Biria[a], Miralena I. Tomescu[a], Anna Custo[a,d], Lucia M. Cantonas[a], Kun-Wei Song[a], Maude Schneider[b], Micah M. Murray[c,d,e,f], Stephan Eliez[b], Christoph M. Michel[a,d], Tonia A. Rihs[a,*]

[a] Functional Brain Mapping Laboratory, Department of Fundamental Neuroscience, University Medical School, University of Geneva, Geneva, Switzerland
[b] Developmental Imaging and Psychopathology Laboratory, Department of Psychiatry, University of Geneva, Geneva, Switzerland
[c] The Laboratory for Investigative Neurophysiology (The LINE), Neuropsychology and Neurorehabilitation Service and Department of Radiology, University Hospital Center and University of Lausanne, Lausanne, Switzerland
[d] EEG Brain Mapping Core, Center for Biomedical Imaging (CIBM) of Lausanne and Geneva, Lausanne, Switzerland
[e] Department of Hearing and Speech Sciences, Vanderbilt University Medical Center, Nashville, TN, USA
[f] Department of Ophthalmology, University of Lausanne, Fondation Asile des Aveugles, Lausanne, Switzerland

ARTICLE INFO

Keywords:
22q11.2 Deletion Syndrome
Schizophrenia
High-density EEG
Biomarkers
Illusory contours
Prodromal symptoms

ABSTRACT

Carriers of the rare 22q11.2 microdeletion present with a high percentage of positive and negative symptoms and a high genetic risk for schizophrenia. Visual processing impairments have been characterized in schizophrenia, but less so in 22q11.2 Deletion Syndrome (DS). Here, we focus on visual processing using high-density EEG and source imaging in 22q11.2DS participants (N = 25) and healthy controls (N = 26) with an illusory contour discrimination task.

Significant differences between groups emerged at early and late stages of visual processing. In 22q11.2DS, we first observed reduced amplitudes over occipital channels and reduced source activations within dorsal and ventral visual stream areas during the P1 (100–125 ms) and within ventral visual cortex during the N1 (150–170 ms) visual evoked components. During a later window implicated in visual completion (240–285 ms), we observed an increase in global amplitudes in 22q11.2DS. The increased surface amplitudes for illusory contours at this window were inversely correlated with positive subscales of prodromal symptoms in 22q11.2DS.

The reduced activity of ventral and dorsal visual areas during early stages points to an impairment in visual processing seen both in schizophrenia and 22q11.2DS. During intervals related to perceptual closure, the inverse correlation of high amplitudes with positive symptoms suggests that participants with 22q11.2DS who show an increased brain response to illusory contours during the relevant window for contour processing have less psychotic symptoms and might thus be at a reduced prodromal risk for schizophrenia.

1. Introduction

The 22q11.2 Deletion Syndrome (22q11.2DS), also known as velocardiofacial or DiGeorge syndrome is the most common microdeletion syndrome that affects up to 1:2000 live births in the United States (Shprintzen, 2008). It is caused by a small deletion in the chromosome 22q11.2 region with a length of 1.5–3 megabases of DNA (Carey et al., 1992; Emanuel, 2008; Hacıhamdioğlu et al., 2015; Scambler, 2000). Its clinical phenotype includes congenital heart disease, palatal abnormalities, facial dysmorphisms (Óskarsdóttir et al., 2005; Yamagishi, 2002) and cognitive deficits (Karayiorgou et al., 2010; Schneider et al., 2014a). The psychiatric profile is characterized by attention-deficit hyperactivity disorder, anxiety and mood disorders and, a marked risk for schizophrenia spectrum disorders (Schneider et al., 2014b).

Notably, children and adolescents with 22q11.2DS frequently present with positive and negative symptoms that are both a hallmark for schizophrenia and appear frequently in its prodromal stage (Debbané et al., 2006; Gourzis et al., 2002; Schneider et al., 2014b). Amongst adults with the 22q11.2 microdeletion, 30% meet (DSM-IV) diagnostic criteria for schizophrenia (Debbané et al., 2006; Schneider et al., 2011) and 40% for schizophrenia spectrum disorders (Schneider et al., 2014a). 22q11.2DS is often diagnosed early in life (Debbané et al., 2005). This allows following individuals through their development and before the onset of schizophrenia. Chromosome 22q is also a susceptibility locus for schizophrenia (Coon et al., 1994; Karayiorgou et al., 2010). For these reasons, the 22q11.2DS can contribute to the search for biomarkers that appear early, in the prodromal stages of schizophrenia (Kates et al., 2012; Schaer et al., 2009), with the aim to

* Corresponding author.
E-mail address: tonia.rihs@unige.ch (T.A. Rihs).

https://doi.org/10.1016/j.nicl.2017.12.028
Received 22 August 2017; Received in revised form 11 December 2017; Accepted 20 December 2017
Available online 21 December 2017

enhance early detection and treatment interventions and ultimately, enable a better prognosis (Fisher et al., 2013; McGlashan and Johannessen, 1996; Miller et al., 1999; Morrison et al., 2007).

Schizophrenia is often characterized by deficits in higher-order cognitive processing (Fioravanti et al., 2005), but perceptual deficits of auditory (Javitt and Sweet, 2015) and visual processing are often downplayed (Silverstein and Keane, 2011). Impairments during the early stages of sensory processing may precede and thus contribute to the higher-order perceptual deficits commonly observed in schizophrenia (Butler et al., 2001; Javitt, 2009; Johnson et al., 2005).

Individuals with schizophrenia show alterations in visual backward masking (Plomp et al., 2013) and also impaired visual contour integration or Gestalt perception (Butler et al., 2013; Silverstein and Keane, 2011; Uhlhaas and Silverstein, 2005). The active process to form a percept of a coherent object based on missing or fragmented visual information is called perceptual closure (Snodgrass and Feenan, 1990) and was also found to be impaired in people living with schizophrenia (Doniger et al., 2002; Sehatpour et al., 2010). Possibly, as a consequence of these impairments, participants with schizophrenia are less prone to see certain visual illusions that rely on size contrast (Ebbinghaus figures) or perceptual organization (Notredame et al., 2014).

Illusory contours (ICs) appear where segregated edges lead to the percept of a shape or contour, in the absence of a physical border (Lesher, 1995). IC's have been related to an active process of “filling-in” of missing information in order to perceive a complete figure or Gestalt percept (law of closure; Kanizsa, 1976). This process was proposed to occur in sequential stages, where a more automatic, filling-in or boundary completion occurs earlier in time and can be segregated from integration to form a shape percept at later stages (Murray et al., 2006). In schizophrenia, the processing of illusory contours per se appears to be preserved (Foxe et al., 2005; Knebel et al., 2011), although performance impairments related to shape integration may be more pronounced in disorganized schizophrenia (Keane et al., 2014). To date, it is not known whether illusory contour processing is more affected in 22q11.2DS compared to schizophrenia.

Event-related potentials (ERPs) are good candidate endophenotypes of cognitive deficits in schizophrenia (Luck et al., 2011; Yeap et al., 2006). Components of the ERPs are defined as time-periods of topographic stability, which is maximal around the peak of the Global Field Power (Michel and Murray, 2011; Michel et al., 2001). The P1 or P100 represents an early cortical response to a visual stimulus. It peaks around 100 ms after stimulus onset and has cortical generators in both the dorsal and ventral visual stream (Di Russo et al., 2002; Murray et al., 2001; Woldorff et al., 1997). The P1 is followed by the N1 or N170, with peak latencies around 160 to 170 ms and generators located predominantly in the ventral visual stream (Allison et al., 1999; Doniger et al., 2001; Shpaner et al., 2013). In illusory contour tasks, the N1 is the first early component, during which a differentiation between contours and non-contours is observed and was related to boundary completion (Foxe et al., 2005, 2001; Murray et al., 2006, 2002; Murray and Herrmann, 2013).

A later component termed Negativity for Closure (Ncl) was first observed when healthy subjects were asked to identify fragmented line-drawings of figures (Doniger et al., 2001, 2000). In these tasks, the Ncl has an onset latency at 230 ms and a peak at 280 ms. It is observed in tasks involving visual completion (Butler et al., 2013; Sehatpour et al., 2010; Shpaner et al., 2013) as well as for illusory contours with a more pronounced amplitude for illusory contours compared to non-contours (Foxe et al., 2005). In a two-stage model of illusory contour processing, this later Ncl response was proposed to be related to a more active and effortful process of shape-discrimination compared to the early-latency N1 modulation (Foxe et al., 2005; Murray et al., 2006, 2002). Sources of the Ncl are predominantly found in the Lateral Occipital Cortex or LOC (Doniger et al., 2001; Sehatpour et al., 2010), a region of the ventral visual stream that was identified as crucial for the recognition of coherent objects (Grill-Spector et al., 2001).

In schizophrenia, reduced amplitudes of the P1 are consistently observed across different visual paradigms (Butler et al., 2013; Doniger et al., 2002; Foxe et al., 2005; Knebel et al., 2011). With regard to the visual N1, some studies find deficits during the N1 component (Johnson et al., 2005; Plomp et al., 2013). However, when investigating illusory contours in schizophrenia, the N1 response to the visual input per se was not significantly reduced and the differentiation between contours and non-contours was also preserved (Butler et al., 2013; Dias et al., 2011; Foxe et al., 2005). During the Ncl in schizophrenia, reduced amplitudes were found for the integration of fragmented figures (Doniger et al., 2002), but increased amplitudes for illusory contours were observed with an aberrant activation of frontal areas (Foxe et al., 2005).

In 22q11.2DS, to our knowledge, neither perceptual closure nor contour perception have been investigated. While not directly related to illusory contour perception, a recent study by Bostelmann et al. (2016) found that children and adolescents with 22q11.2DS produced more errors in object memory than spatial memory tasks, which might point to a more pronounced impairment in ventral stream processing (Bostelmann et al., 2016). Neuroimaging studies in 22q11.2DS during rest show structural and functional alterations in regions important for visual processing, with decreased cortical thickness over superior parietal and parieto-occipital regions in children and young adults (Schaer et al., 2010) and reduced functional connectivity in parietal, temporal and left occipital lobes in adolescents and young adults with this syndrome (Scariati et al., 2014).

In the present study, visual processing during illusory contour detection in 22q11.2DS was compared to typically developing adolescents and adults. More specifically, using high-density EEG, we investigated whether we would find alterations of amplitude and source activity during the P1 and N1 components in 22q11.2DS that are consistent with findings of reduced activation of early visual components seen in schizophrenia and, whether we would observe evidence for altered illusory contour sensitivity in 22q11.2DS during the N1 and Ncl windows.

2. Methods

2.1. Participants

For this cross-sectional study, we analyzed participants, aged between 14 and 28 years that were enrolled by the Department of Psychiatry at the Developmental Imaging and Psychopathology Laboratory in Geneva, Switzerland, as part of the Geneva cohort investigation on 22q11.2DS. The 22q11.2DS participants and controls were recruited through announcements in patient associations in Switzerland, Belgium and France as well as through local announcements in Geneva. Controls were community controls or siblings of the 22q11.2DS participants without the deletion. All participants signed an informed consent approved by the Local Research Committee, the Commission Centrale d'Ethique de la Recherche (CCER) in Geneva, Switzerland in accordance with the code of Ethics of the World Medical Association (Declaration of Helsinki). Parents signed the informed consent for participants younger than 18 years old. The presence of a deletion in chromosome 22q11.2 was confirmed by Quantitative Fluorescent Polymerase Chain Reaction (QF-PCR).

The binocular vision of all participants was assessed using the Freiburger Acuity Test (Bach, 2007). Moreover, to ensure that all our participants were able to perform the main task, we only included participants with accuracy rates above 65% in the Kanizsa task. From the initial 22q11.2DS group (N = 49), two participants were eliminated due to low performance levels and two were excluded due to missing behavioral data. Initially, 45 participants with 22q11.2DS and 31 control subjects met the inclusion criteria and their EEG data were analyzed. Eighteen participants with 22q11.2DS and five control participants had to be excluded from further analysis due to excessive

Table 1
Clinical sample description.

	22q11.2DS	Controls
N	25	26
Age (mean age ± std)	19.6 ± 3.4	17.8 ± 3.3
Gender (f/m)	13/12	8/18
FSIQ (mean ± std)*	73.4 ± 10.5	112.4 ± 13.1
ADHD	6	0
Anxiety disorders	9	0
Mood disorders	5	0
Psychotic disorders	4	0
Antipsychotic treatment	4	0
Antidepressant treatment	3	0
Cardiac malformations	9	0
PANSS, positive (T-score, mean ± std)	37.6 ± 10.2	NA
PANSS, negative (T-score, mean ± std)	48.4 ± 11.1	NA
PANSS, general (T-score, mean ± std)	41.8 ± 12.1	NA

Note: Diagnoses were based on Diagnostic Interview for Children and Adolescents (DICA-IV; Reich, 2000), using either *DSM-IV* or *DSM-III-R* criteria. Adult participants were screened using the Structured Clinical Interview for DSM-IV axis I disorders (SCID-I; First et al., 1996). Four of the participants with 22q11.2DS showed comorbidities between psychotic disorders, anxiety disorders and mood disorders. One participant was prescribed both antipsychotic and antidepressant medications. Of the 9 participants with cardiac malformations, 6 underwent invasive cardiac surgery during childhood. PANSS: Positive and Negative Symptoms Scale (Kay et al., 1987). Raw scores were converted to T-scores using the PANSS manual.

* FSIQ: Full scale IQ was significantly lower in 22q11.2DS compared to controls [$t_{(49)} = 11.6$, $p < 0.001$].

amounts of eye blinks, movement and noise in the EEG data.

25 participants with 22q11.2DS (13 females, 12 males; mean age ± std: 19.62 ± 3.38, median age: 19, range: 14–25 years) and 26 healthy controls (8 females, 18 males; mean age ± std: 17.88 ± 3.31, median age: 18, range: 14–28 years) were included in the final analysis. An independent samples *t*-test showed no significant difference between the two groups for age [$t_{(49)} = -1.88$, $p > 0.05$] and a Chi-square test showed no significant differences for gender [$\chi^2(1, N = 51) = 2.37$, $p > 0.05$] between the two groups.

2.2. Clinical assessment

All 22q11.2DS participants younger than 18 years old were screened with the Diagnostic Interview for Children and Adolescents (DICA-IV; Reich, 2000). Adult participants were screened using the Structured Clinical Interview for DSM-IV axis I disorders (SCID-I; First et al., 1996). One out of 25 participants received a diagnosis of schizophrenia and 3 more participants were diagnosed with a psychotic disorder. Demographic and clinical variables are shown in Table 1.

The intensity of psychotic manifestations in 22q11.2DS was assessed by a psychiatrist (S.E.) through an interview with the parent/caregiver and the participant. All 22q11.2DS participants were evaluated with the Positive And Negative Symptom Scale (PANSS; Kay et al., 1987); see Table 1. Participants were also screened with the symptom scale of the Structured Interview for Psychosis-Risk Syndromes (SIPS, McGlashan et al., 2001; Miller et al., 2003). The SIPS uses a 7-point severity scale to assess positive, negative, disorganization and general prodromal symptoms (ranging from 0 to 6). Table 2 shows the number of participants presenting with prodromal symptoms as measured by the SIPS.

All participants were tested on a full Wechsler Intelligence scale for children III-R, or IV (WISC-III-R/WISC-IV) or the Wechsler Adult Intelligence Scale-III or IV (WAIS-III/WAIS-IV) for participants older than 17 years old. There were significant differences between the two groups on the Full-scale IQ (FSIQ) as shown by an independent sample *t*-test on the FSIQ: [22q11.2DS; mean ± S.D.: 73.4 ± 10.47; control group; mean ± S.D.: 112.36 ± 13.12; $t_{(49)} = 11.6$, $p < 0.001$] see Table 1.

Table 2
Prodromal symptoms of 22q11.2DS participants, SIPS scale.

Prodromal symptoms	Positive	Negative	Disorganization	General
Moderate to severe (3–6)	12	21	11	10
Questionably present to mild (1–2)	8	4	14	14
Absence of symptoms (0)	5	0	0	1

Note: Prodromal symptoms were evaluated based on the symptom scale of the Structured Interview for Prodromal Symptoms (SIPS; McGlashan et al., 2001; Miller et al., 2003) in all 25 participants with 22q11.2DS.

2.3. Stimuli and task

Participants were instructed to keep their gaze on a central fixation point while arrays of 4 “pac-man” inducers were presented. The pac-man shapes were oriented to either form an illusory contour (IC) or a non-contour (NC) (see Fig. 1). Moreover, the inducers were positioned either on the cardinal or diagonal axes so as to form ICs of circles or squares, respectively (e.g., Knebel et al., 2011). These variations were included to minimize the likelihood that participants could retain their gaze or attention at one location to successfully perform the task. The inducers were presented on a CRT computer monitor with a 70 Hz refresh rate that was located 1 m from the participant and appeared white on a black background. The stimuli were administered using the program E-Prime (E-prime version: 1.2.1.17; Psychology Software Tools, Inc., Pittsburgh, USA; www.pstnet.com/eprime; Schneider et al., 2002).

Both circle and square shapes had visual angles (θ) of 3.093° for the inner and 4.352° for the outer imaginary boundaries in both the vertical and horizontal plane. The inner angle was measured by the imaginary diameter of the circle or contour line of the square on the horizontal or vertical plane (D) and the distance from the screen (S). The outer angle was obtained by taking the imaginary line of the outer perimeter created by the pac-man inducers and the distance from the screen (S). The radius of the pac-man inducer circles had a visual angle of 1.260°. Visual angles (θ) were computed using the following formula $\theta = 2 * \text{atan}((S / 2) / D)$.

The task was split into three blocks of approximately three minutes duration. The four different stimuli were presented for 500 ms in a random sequence with a repetition of 25 times for each stimulus within each run (total of 75 repetitions per stimulus and 150 repetitions per condition). The inter-stimulus interval varied randomly between 800 and 1200 ms, during which participants had to fixate the white dot on a full screen black background. A response pad was located in front of the participant with four buttons indicating the numbers from one to four from left to right. Subjects were instructed to press the number one key with the index finger of their right hand when they identified the illusory contour and the number two key when the illusory contour was absent, using the middle finger of the same hand. All subjects underwent a trial run before starting the experiment to ensure that they understood the task and instructions. These instructions were explained before the trial run and re-iterated before the first run. The task instructions were also present as a text slide before each run. Reading of instructions and visual fixation of the screen during the experiment was ensured by continuous video monitoring of the participant by the experimenters.

2.4. Behavioral analysis

The performance of all participants was evaluated using the reaction time (RT) and accuracy of the responses. Two mixed-design analyses of variance (ANOVA's) were used to compare the median RTs in milliseconds and percentage accuracies between groups and conditions with the R studio software (R Core Team, 2013) and the factors group (controls vs. 22q11.2DS) and condition (IC vs. NC). Further, to investigate a potential speed-accuracy tradeoff, the Inverse Efficiency

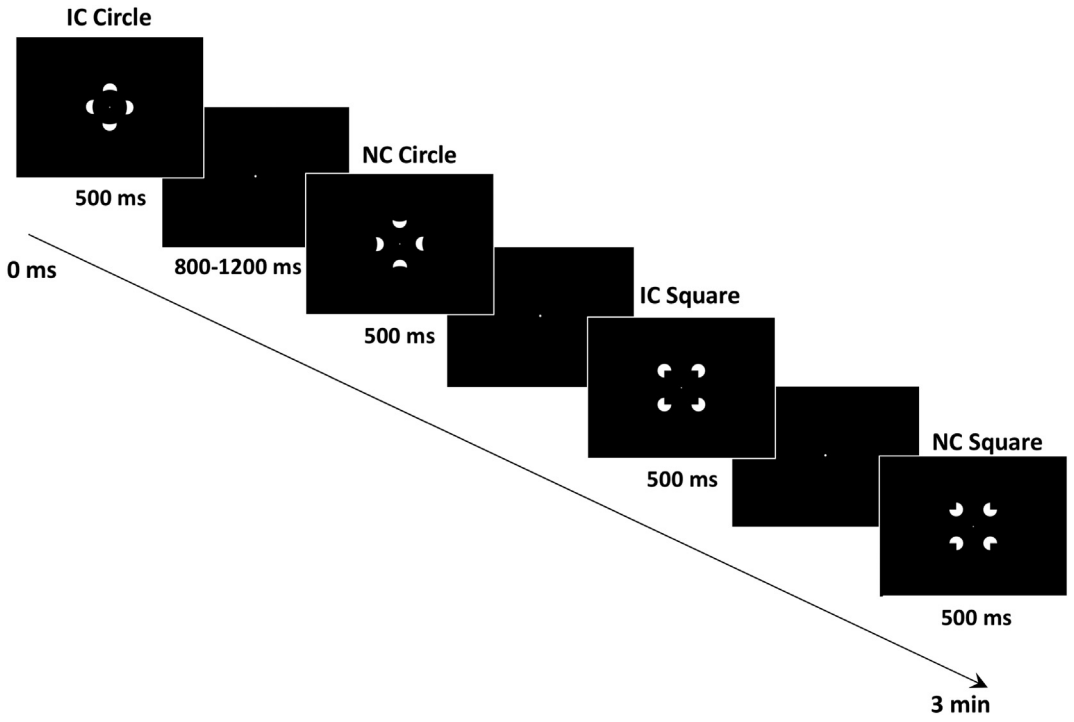

Fig. 1. Task.
The first and third images show the circle and square illusory contour (IC) trials. The second and last images show the circle and square non-contour (NC) trials. Both IC and NC conditions were equally (25%) and randomly distributed within each run of the task. The duration of every run was 3 min with three runs in total. Participants were required to indicate by a button press on a response box whether they identified an illusory contour or not (non-contour condition).

Scores (IES) were calculated by dividing the median RT by the percentage of correct responses for each participant and condition (Akhtar and Enns, 1989; Christie and Klein, 1995). Next, a mixed-ANOVA was performed for both groups and conditions using the IES as dependent variable.

2.5. EEG recording

During the EEG recording, participants were sitting in a comfortable, upright position in an electrically shielded room and were instructed to stay as calm as possible. Continuous EEG was recorded through high-density EEG with a 256-channel hydrocel cap (Electrical Geodesics Inc., Eugene, OR, USA). Impedance measures were kept below 30 kΩ. Signal quality was monitored between recording blocks by impedance measurements. A sampling rate of 1000 Hz and a vertex reference at electrode Cz were used to acquire the data.

2.6. ERP preprocessing

Once the data were acquired, the electrodes located on the cheek and nape were excluded and the remaining 204 electrodes were kept for further analysis. Offline data processing was performed with the Cartool software (https://sites.google.com/site/cartoolcommunity). Data were high-pass and low-pass filtered between 1 and 40 Hz (causal filtering, DC removed, 24db/octave roll-off). The epochs were averaged from -200 ms before to + 600 ms post-stimulus onset to compute the visual evoked potentials (VEPs). During this step, trials contaminated with eye blinks and movements were rejected based on visual inspection. To yield a better signal to noise ratio, the two contour stimuli were averaged together, as well as the two non-contour stimuli. The potentials from artifact electrodes were interpolated at the single subject level (Perrin et al., 1989). The data were then average-referenced and downsampled to a sampling rate of 250 Hz for further analysis. The result of a mixed-design ANOVA showed no significant differences ($p > 0.05$) in the epoch acceptance rates between groups and conditions (mean ± S.D.: in 22q11.2DS: IC: 76.92 ± 26.38, NC: 76.08 ± 25.24; in controls: IC: 76.73 ± 24.70, NC: 75.69 ± 22.93).

2.7. EEG surface analysis

The first step of the VEP analysis consisted of an identification of the main components of interest for this analysis, namely the P1, the N1 and the Ncl components. The components were identified by their Global Field Power peak and the topography. GFP peaks were found in both groups for the P1 between 100 and 125 ms, for the N1 between 150 and 170 ms and for the IC condition during the Ncl between 240 and 285 ms. The signals within these three windows of interest (P1, N1 and Ncl) were averaged and randomization tests were performed for the Global Field Power (GFP). The Global Map Dissimilarity (GMD) was investigated with the Topographic Analysis of Variance (TANOVA). Both randomized tests were performed using the within subject factor condition (IC vs. NC) and the between subjects factor group (controls vs. 22q11.2DS). The Global Field Power (GFP) measures the strength of the scalp potential field and is calculated as the standard deviation across all electrodes at a given timepoint (Brunet et al., 2011; Lehmann and Skrandies, 1980). The individual subject GFPs were compared between the two groups and conditions using a permutation statistic with 5000 iterations. To investigate the field topography differences between groups and conditions, the Topographic Analysis of Variance (TANOVA) was performed. This is a randomization test to compare the Global Map Dissimilarity (GMD) values to investigate topographic differences of scalp potential maps (Murray et al., 2008). For all permutation tests on the surface, a significance level of $p < 0.05$ and 5000 iterations were fixed. These parts of the analysis were performed with the Ragu software (Koenig and Melie-Garcia, 2010). In addition, paired randomized analyses were performed for the amplitudes on each electrode to characterize the between group differences and between condition differences for the three windows of interest at the electrode level. For the permutation tests on the surface amplitudes, a significance level of $p < 0.05$ and a temporal criterion of at least 10

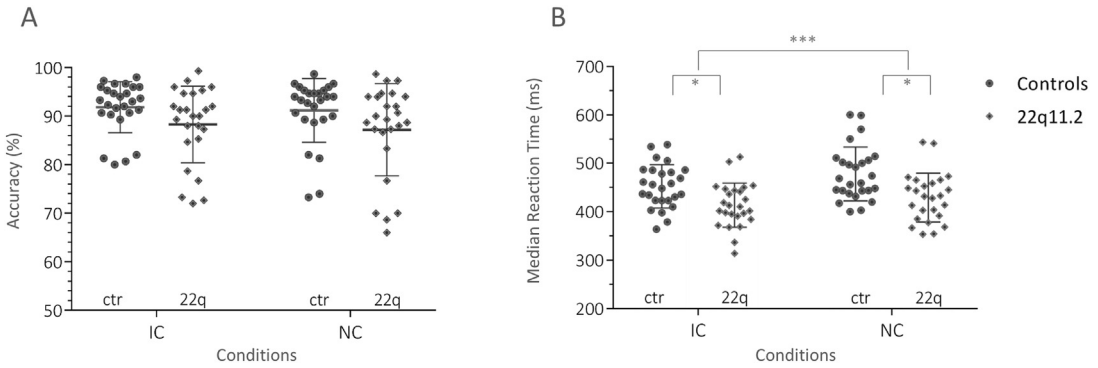

Fig. 2. Behavior: accuracy and median reaction times per group and condition.
(A) Scatter dot plot for the percentage accuracy for both groups (22q11.2DS vs. Controls) and conditions: Illusory contours (IC) vs. Non-Contours (NC). Error bars indicate the standard deviation from the mean. (B) Scatter dot plot for the median reaction times for both groups (22q11.2DS vs. Controls) and conditions: Illusory contours (IC) vs. Non-Contours (NC). Error bars indicate the standard deviation from the mean. The significance levels of $p < 0.01$ and $p < 0.0001$ are indicated with one and three stars respectively. The diamond shapes in grey represent the 22q11.2DS participants and the darker circles represent controls in both plots.

milliseconds of significance were fixed, meaning that the threshold significance level of 5% had to be maintained for a minimal duration of 10 ms. This analysis was performed with the Cartool software (https://sites.google.com/site/cartoolcommunity).

2.8. ERP correlations with clinical data

A Pearson product-moment correlation coefficient analysis was performed with the R studio software (R Core Team, 2013) to investigate the associations between the clinical symptom scores (SIPS and PANSS) for the 22q11.2DS participants and their Event Related Potential (ERP) data measured on the surface. For this purpose, the GFP time windows corresponding to the visual evoked potential components (P1, N1 and Ncl), were selected if a clear GFP peak was detectable in the time-window. Next, the areas of the components were calculated for each individual subject and used as the input for the correlation coefficient analysis along with the clinical test scores of the SIPS and PANSS. For the correlations between clinical symptoms and the area below the GFP during the Ncl time-window, only the IC condition was taken into account. In contrast to controls, the signal of the NC condition in 22q11.2DS during the Ncl window did not allow to identify a GFP peak and corresponding topography at the single subject level and was thus not used for the correlation analysis. For the P1 and N1, both conditions were considered. Differences were considered significant when *p*-values were smaller than 0.05.

2.9. EEG source analysis

In the next step of analysis, the sources of the ERPs were estimated for each subject using the linear distributed inverse solution, LAURA, for Local Auto-Regressive Averages (Grave De Peralta Menendez et al., 2004). The lead field for the inverse solution was calculated for 204 electrode positions and the average brain of the Montreal Neurological Institute in a grey matter constrained head model using a modified version of the Spherical Model with Anatomical Constraints head model (SMAC, Spinelli et al., 2000) with 5018 distributed solution points (Brunet et al., 2011).

To obtain values for the significance of the source activity, the Topographic Electrophysiological State Source-imaging method (TESS, Custo et al., 2014) was used to localize the neuronal generators of the scalp electrical activity using LAURA, for time-locked states of interest. TESS is based on a two-step general linear model (GLM) fitting and is designed to estimate the sources, and their statistical significance, for a set of states identified in the EEG recordings which correspond to the time windows of interest (P1, N1 and Ncl). The method works as follows: first, the number of epochs (N) per subject and condition (controls: IC: mean epochs (76.73, range: 30–133), controls NC: mean epochs (75.69, range: 30–111); 22q11.2 for IC mean epochs (76.92, range: 37–132), 22q11.2 NC mean epochs (76.08 range: 36–135) are projected into inverse space using LAURA. We generated a set of three regressors as index functions (iff) over the time periods of interest (index_1(t) = 1 iff t = 100–125 ms, 0 otherwise; index_2(t) = 1 iff t = 150–170 ms, 0 otherwise; index_3(t) = 1 iff t = 240–285 ms, 0 otherwise). A general linear model (GLM) was then used to estimate the coefficients to best linearly fit the three regressors to the data (the N epochs). Finally, we estimated the statistical significance ($p < 0.01$, Bonferroni-corrected) of the GLM coefficients via contrast analysis (testing for group effect, condition effect, or the combined effect of group and condition for each of the three latencies). The contrast analysis was performed using SPM12 [http://www.fil.ion.ucl.ac.uk/spm/software/spm12/] and MATLAB (version R2014a).

3. Results

3.1. Behavior: accuracy and median reaction time

To study the effect of group and condition on the median RT and accuracy of the responses, two mixed-design ANOVA's were performed with the factors group (22q11.2DS vs. Controls) and condition (IC vs. NC).

The ANOVA for accuracy did not yield a significant main effect of group [mean ± S.D.; 22q11.2DS: 87.75 ± 8.67%; controls: 91.50 ± 5.90%, n.s.], nor condition [mean ± S.D.; IC: 90.09 ± 6.85%; NC: 89.22 ± 8.31%, n.s.]. Further, no significant interaction was found between group and condition for accuracy. Fig. 2A shows the accuracy bar plot for the two groups.

The ANOVA on median reaction times revealed a significant main effect of condition, indicating that both groups were significantly faster in the illusory contour (IC) present condition compared to the non-contour (NC) condition [median RT: mean ± S.D.; IC: 434.5 ± 48.8 ms; NC: 445 ± 58.0 ms, $F_{(1,49)} = 24.18$, $p < 0.0001$, $\eta_G^2 = 0.044$]. The main effect for group was also significant with 22q11.2DS participants being significantly faster than controls [median RT: mean ± S.D.; 22q11.2DS: 416.5 ± 48.18 ms; controls: 457 ms ± 51.6 ms, $F_{(1,49)} = 11.16$, $p < 0.01$, $\eta_G^2 = 0.17$]. There was no significant interaction between group and condition for the median reaction time (see Fig. 2B).

Moreover, in a mixed ANOVA, the inverse efficiency scores (IES) yielded a significant main effect of condition [IES: mean ± S.D.: IC: 4.83 ± 0.58; NC: 5.13 ± 0.79; $F_{(1,49)} = 15{,}7379$, $p < 0.001$]. The main effect of group and the interaction were not significant.

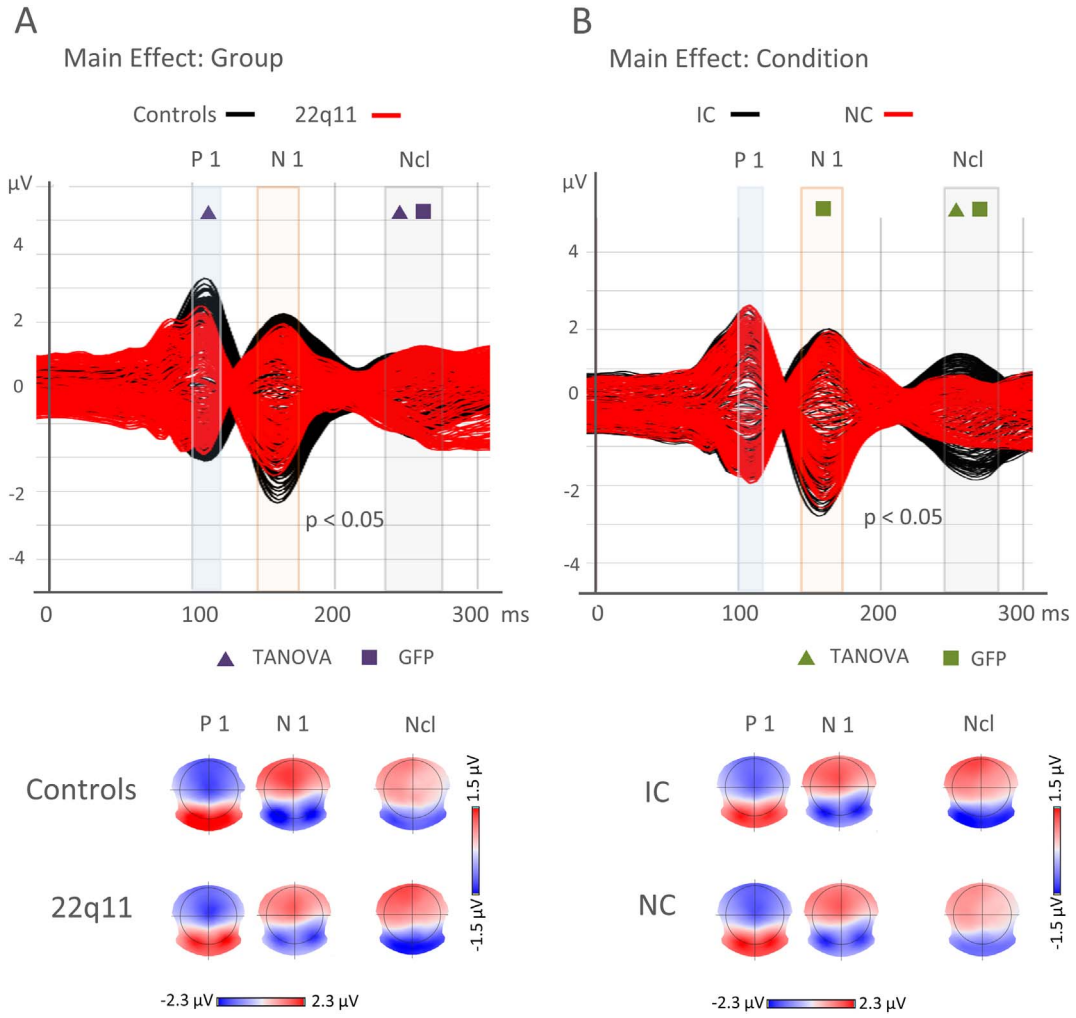

Fig. 3. Surface EEG for the main effects of group and condition.
(A) Main Effect Group: Superimposed EEG traces per group (controls vs. 22q11.2DS). Controls are shown in black and participants with 22q11.2DS in red. The transparent frames indicate time windows of the components of interest, the P1 (100–125 ms) in blue, the N1 (150–170 ms) in light red and the Negativity for Closure (Ncl: 240–285 ms) in grey. Significant differences for the main group effect of the randomized test for the GFP are shown with a purple square, for the Topographic Analysis of Variance TANOVA with a purple triangle. A significance level of $p < 0.05$ was to be maintained. Below the traces, the corresponding topographical maps of the group averages for the controls and 22q11.2DS groups are shown during the P1, the N1 and the Ncl time window.
(B) Main Effect Condition: Superimposed EEG traces for the Illusory Contour (IC) in black and the Non-Contour (NC) condition in red. The transparent frames indicate time windows of the components of interest, the P1 (100–125 ms) in blue, the N1 (150–170 ms) in light red and the Negativity for Closure (Ncl: 240–285 ms) in grey. Significant differences for the main effect of condition of the randomized test for the GFP are shown with a green square, for the Topographic Analysis of Variance TANOVA with a green triangle. A significance level of $p < 0.05$ was to be maintained. Below the traces, the corresponding topographical maps of the condition averages for the IC and NC condition are shown during the P1, the N1 and the Ncl time window.

3.2. EEG surface analysis

Spatial analysis: When investigating differences in topography with the TANOVA for the averaged P1 window (100–125 ms), the main effect of group was significant ($p = 0.001$). No significant effect for condition was found during the P1 window ($p = 0.845$). No significant TANOVA main effect for group or condition was found during the N1 window (150–170 ms). The TANOVA for the Ncl window showed a significant effect for group ($p = 0.024$) and condition ($p = 0.029$) and no significant interaction.

Global field strength analysis: The randomization test comparing the Global Field Power (GFP) for the averaged time windows of the P1 (100–125 ms) found no significant effect for group nor condition. During the N1 (150–170 ms), the condition main effect was significant ($p = 0.03$), but no significant group effect or interaction were found. For the Ncl window (240–285 ms), a highly significant main effect was found for condition ($p = 0.0002$) and group ($p = 0.039$) with higher GFP for the IC condition and in the group with 22q11.2DS. The interaction was not significant.

As can be seen in the waveforms and topographic maps of Fig. 3A, participants with 22q11.2DS showed a general decrease in amplitude during the P1 (100–125 ms) and N1 (150–170 ms) compared to the control subjects. However, compared to controls, the NC condition in 22q11.2DS group did not yield a clear peak during the Ncl time window. While on a global level (TANOVA), only the effect on the P1 reached significance, a randomization test on the electrode amplitudes showed significant differences for all timepoints of the P1 and the N1 windows ($p < 0.05$). For the P1 and N1 time windows, significantly lower amplitudes were found for occipital, parietal and posterior temporal sensors in 22q11.2DS compared to controls, while the amplitudes over frontal and anterior temporal electrodes were increased in those intervals in 22q11.2DS participants, compared to controls. These results indicate that initial and late stages of visual processing were characterized by distinct configurations of intracranial generators in each group.

In contrast to the lower GFP and occipital amplitudes for the P1 [GFP,

P1: mean ± S.D.; 22q11.2DS: 2.69 ± 0.18 μV; controls: 2.78 ± 0.18 μV], the GFP amplitudes during the Ncl were higher in the 22q11.2DS group compared to control subjects [GFP, Ncl: mean ± S.D.; 22q11.2DS: 2.36 ± 0.18 μV; controls: 1.90 ± 0.09 μV]. This was shown by the randomized GFP analysis that yielded significant group differences during this time window. In addition, the randomization test over all electrodes demonstrated significantly higher positive amplitudes over frontal electrodes and increased negativity over occipital electrodes for the 22q11.2DS group compared to controls.

Fig. 3B shows the superposed amplitudes of the two conditions as well as the topographic maps corresponding to the three windows of interest. In the randomized analysis of the GFP, there was a main effect for condition during the N1 [GFP, N1: mean ± S.D.; IC: 3.1 ± 0.08 μV; NC: 2.81 ± 0.12 μV] and Ncl [GFP, Ncl: mean ± S.D.; IC: 2.38 ± 0.09 μV; NC: 1.87 ± 0.05 μV] components with higher GFP amplitudes for the IC condition both during the N1 and Ncl windows. The paired randomized tests for amplitude values revealed higher negative values over occipital electrodes and also higher positive amplitude values over fronto-central electrodes for the Ncl window.

The comparison of the spatial analysis by means of the TANOVA revealed a main effect for condition during the Ncl window. This indicates that both groups dissociated between illusory contours and non-contours and that this dissociation was found to be strongest during the Ncl window.

3.3. ERP correlations with clinical data

Within the 22q11.2DS group, a Pearson product-moment correlation coefficient analysis detected no significant correlations between amplitudes of the GFP during the P1 and N1 components and the scores on the subscales of the PANSS and SIPS scales ($p > 0.05$). However, the GFP amplitude of the IC condition during the Ncl time window (240–285 ms) was inversely correlated with the positive subscales of the PANSS, r (25) = −0.51, $p = 0.01$ and SIPS, r (25) = −0.58, $p = 0.002$.

3.4. EEG source imaging

We selected the time periods during the P1 (100 ms–125 ms), N1 (150 ms–170 ms), and Ncl (240 ms–285 ms). Then we estimated the active sources in these time windows using TESS (Custo et al., 2014). A significance level of $p < 0.01$ and a Bonferroni correction were used. In the next step, a contrast analysis was performed between both groups and conditions. During the P1 component (100–125 ms), the 22q11.2DS group showed significantly lower activations over bilateral precunei, lingual gyri, posterior cingulate and the left parietal lobe (Fig. 4A). Higher activation for 22q11.2DS was found bilaterally at the Anterior Cingulate Cortex (ACC), the medial frontal gyri, cingulate gyri, thalamus, right temporal gyrus and left medial frontal gyrus when compared to control participants (Fig. 4B).

When comparing the two groups with TESS for the N1 time window (150–170 ms, single trial analysis), the control group activated the cuneus, precuneus, middle temporal lobes, occipital lobes, and posterior cingulate bilaterally and significantly more than the patient group (Fig. 4C). The 22q11.2DS group showed higher bilateral activations at the ACC, cingulate gyri, inferior, medial, and middle frontal gyri, thalamus, and insula (Fig. 4D). In the Ncl time window (240–285 ms), the control group activated the right inferior parietal lobe more than patients (Fig. 4E). During the Ncl window the group with 22q11.2DS showed more activity in the lingual gyrus, cuneus as well as in the left inferior frontal gyrus compared to controls (Fig. 4F).

The contrast for condition during the Ncl showed that both groups have higher activation in the left lingual, fusiform, inferior occipital, and middle temporal gyri in response to illusory contours, when compared to the non-contour condition (Fig. 5A and B). However, the 22q11.2DS group activated a slightly smaller region in the fusiform gyrus compared to control participants.

4. Discussion

In this study, we compared visual processing between participants with 22q11.2DS and a healthy control group. We focused particularly on visual processing during the P1 (Butler et al., 2013; Doniger et al., 2002; Foxe et al., 2005; Knebel et al., 2011), N1 (Johnson et al., 2005; Plomp et al., 2013) and the Ncl components (Doniger et al., 2002) of the visual evoked potential, which are reported to be impaired in patients with schizophrenia across different visual paradigms. In schizophrenia, illusory contour completion was comparable to controls with higher amplitudes for contour compared to non-contour stimuli during the N1 and Ncl components (Foxe et al., 2005; Knebel et al., 2011). Given the high risk profile for schizophrenia in 22q11.2DS, we expected to see similarities in the pattern of ERP responses and source activities between participants with schizophrenia and 22q11.2DS for visual- and illusory contour processing and found that in 22q11.2 DS, illusory contour completion was indeed preserved.

However, the present study reveals significant deficits at earlier timepoints of visual processing, where the P1 component in the group with 22q11.2DS shows a reduction in amplitude over occipital electrodes. At the cortical source level, we found reduced activity over dorsal and ventral visual stream areas, including the lingual gyri and bilateral precunei. In schizophrenia, the P1 surface amplitude and the activation of ventral and dorsal visual stream areas are reduced compared to healthy individuals (Doniger et al., 2002; Foxe et al., 2005; Knebel et al., 2011), pointing to a decreased activation of visual cortices at this early latency that is also observed in 22q11.2DS.

The 22q11.2DS group also showed reduced signal strength over occipital electrodes during the N1. The source analysis during this time window confirmed that activity in the cuneus, precuneus, middle temporal lobes, occipital lobes and posterior cingulate was substantially decreased in 22q11.2DS. In patients with schizophrenia, there are discrepant findings related to the visual N1 component. In studies of illusory contour processing and contour integration, no significant differences between participants with schizophrenia and healthy controls were found for the N1 amplitudes (Butler et al., 2001; Doniger et al., 2002; Foxe et al., 2005; Knebel et al., 2011). Conversely, reduced activations during the N1 were found in a global versus local task (Johnson et al., 2005), a visual go-no go task with centrally presented letters (Oribe et al., 2013) and a visual backward masking paradigm with small Vernier offsets (Plomp et al., 2013). Although these tasks differ from the illusory contour perception task used in this study, they point to impaired processing at the N1 latency in schizophrenia under certain conditions. Related to illusory contour processing, and in accordance with previous research (Foxe et al., 2005; Knebel et al., 2011), 22q11.2DS participants showed a preserved differentiation between the illusory contour and the non-contour stimulus, despite a decrease in N1 amplitudes over occipital electrodes. The intact differentiation between contour and non-contour stimuli appears thus to be present both in 22q11.2DS and schizophrenia during the N1 component and corroborates previous findings of an intact early illusory contour differentiation at this latency (Foxe et al., 2005; Knebel et al., 2011).

The present study found increased GFP amplitudes in the time window of the closure negativity (Ncl) component in the 22q11.2DS group relative to controls. This activity was increased both with a stronger occipital negativity and frontal positivity for illusory contours in 22q11.2DS. Interestingly, in a previous study on Kanizsa illusory contour processing, during the Ncl, patients with schizophrenia showed increased amplitudes that were related to increased activation over frontal cortical areas. The authors concluded that this frontal activity observed in schizophrenia was related to a more effortful conceptual processing (Foxe et al., 2005). It is thus possible, that the increases in frontal activity in 22q11.2DS that were found during early stages (P1 and N1) reflect an increased recruitment of frontal structures to compensate for reduced activity over visual cortices. Interestingly, the EEG response to the non-contour stimuli at the Ncl does not yield a clear ERP

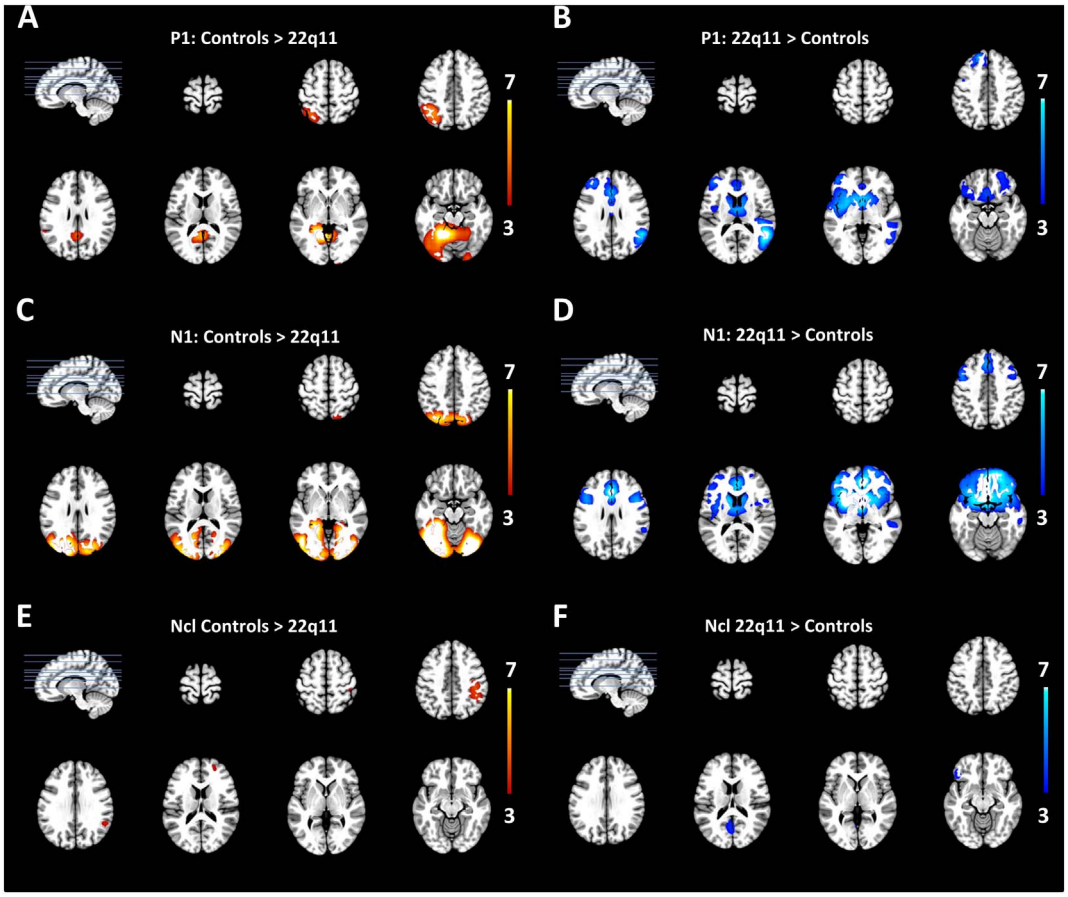

Fig. 4. Between group (22q11.2DS vs. Controls) contrasts of the inverse source space.
Differences in source activity result from single trial analyses using the general linear model (TESS) with a *p*-value < 0.01. The colour bars indicate the T-values. Areas that are significantly more activated in the control group are indicated in orange and areas that were significantly more active in 22q11 participants in blue. (A) The contrast analysis for controls > 22q11.2DS during the P1 (100–125 ms) shows precunei, lingual gyri, posterior cingulate and left parietal lobe. (B) The contrast 22q11.2DS > controls during the P1 shows increased activation over Anterior Cingulate Cortex (ACC), medial frontal gyri, cingulate gyri, thalamus, right temporal gyrus and left medial frontal gyrus. (C) For the N1 window (150–170 ms) the contrast controls > 22q11.2 DS shows more activity in cuneus, precuneus, middle temporal lobes, occipital lobes and the posterior cingulate. (D) Regions significantly more active in 22q11.2DS are the ACC, cingulate gyri, inferior, medial, and middle frontal gyri, thalamus and insula. (E) During the Ncl window, in controls, an area in the right inferior parietal lobe showed more activity compared to the group with 22q11.2DS. (F) In 22q11.2 the regions that showed more activity compared to controls during the Ncl were the Posterior Cingulate Gyrus, the lingual gyrus, the cuneus and the precuneus.

peak in 22q11.2DS. This could also point to specific perceptual processing differences in 22q11.2DS, where the identification of the illusory contour was present but the identification of the non-contour stimulus showed more variability. Alternatively, this finding could also point to a difficulty with local processing in 22q11.2DS. A study by Giersch et al. (2014) found that individuals with 22q11.2DS showed impaired local and not global visual processing in a behavioral task (Giersch et al., 2014). It is thus possible that the lack of a clear evoked component for the non-contour stimuli in 22q11.2DS could partly result from a slight impairment with local visual processing. However, we did not find any significant interaction during this window and the behavioral results for the NC condition in 22q11.2DS do not indicate a particular impairment with identifying the non-contour stimuli. Furthermore, the design of the present study does not allow us to explore the distinction between local and global processing any further. Nonetheless, in accordance with Giersch et al. (2014), it points to

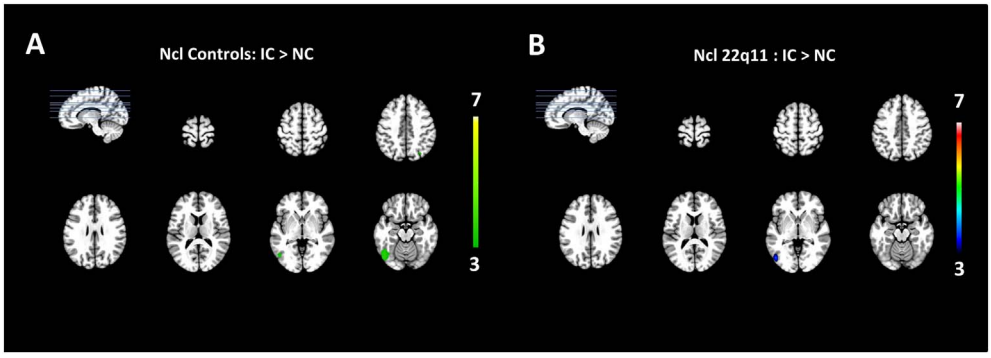

Fig. 5. Between condition (IC vs. NC) contrasts of the inverse source space.
Differences in source activity result from single trial analyses using the general linear model (TESS) with a *p*-value < 0.01. The colour bars indicate the T-values.
The contrast analysis between the two conditions (IC vs. NC) is shown during the Ncl time window (240–285 ms). In controls (A) and 22q11.2DS participants (B) areas that are significantly more active in the IC compared to the NC condition include the left lingual, fusiform, inferior occipital and middle temporal gyri. The green and colour spectrum bar represent areas that were significantly more activated for the IC > NC contrast in controls (A) and 22q11.2DS (B) respectively.

preserved global processing for illusory contour integration in 22q11.2DS.

Another explanation could stem from the observation that spatial processing, visuo-spatial memory and spatial attention (Antshel et al., 2008; Bearden et al., 2001; Shapiro et al., 2012; Simon, 2008) are often found to be impaired in children with 22q11.2DS. In healthy populations, illusory contour configurations were found to strongly capture visual attention (Senkowski et al., 2005). It could thus be possible that even for our participants with 22q11.2DS that were older than 14 years old, the illusory contour stimuli might have led to a reduced attention capture, which could result in more effortful spatial processing and increased early activation of frontal cortices during the P1 and N1 latencies.

The EEG source analysis also identified increased activity in the lateral occipital cortex (LOC) in response to illusory contour perception in contrast to non-contour perception. This activation was comparable to the activity shown by the control group during the Ncl and points to a preserved shape integration in 22q11.2DS.

Since patients were significantly faster than the control group, we investigated the inverse efficiency scores (IES) for associations between reaction time and accuracy of the responses for both groups and conditions. The IES did not differ significantly between groups but showed an effect for the condition, which indicated that in the NC condition, both groups had slower reaction times and lower accuracies. The faster reaction times in 22q11.2DS could thus not be explained by a speed accuracy trade-off in 22q11.2DS.

When investigating the relationship between the EEG findings and clinical symptoms, a significant inverse correlation was detected between positive symptoms of psychosis measured by the positive subscales of the PANSS and SIPS and the Ncl amplitude: the higher the GFP for illusory contours during the Negativity for Closure time window, the lower the positive symptoms. This may suggest that participants with 22q11.2DS who have a lower risk for schizophrenia might respond by an increased and compensatory response for illusory contours during this time window compared to controls.

Despite a high percentage of disorganized symptoms in our participants with 22q11.DS, we did not find significant correlations between disorganization and our EEG markers. In schizophrenia, the disorganization dimension was found to be related to impaired perceptual integration (Keane et al., 2014; Silverstein and Keane, 2011; Uhlhaas et al., 2006). However, in a Kanizsa type task, there was no difference between groups for contour filling-in but for a more difficult task that was probing global shape integration (Keane et al., 2014; Silverstein and Keane, 2011). It is thus possible that the task used in the present study was not sensitive enough to the disorganization dimension.

In 22q11.2DS, the higher activity of the ACC, DLPFC and mPFC appears very early in time during the P1 and N1, while in patients with schizophrenia increased inferior frontal activations were found later, during the Ncl time window (Foxe et al., 2005). In patients with schizophrenia, the ACC and DLPFC are found to be less active than in healthy participants. This was observed in a visual task of global versus local visual processing (Silverstein et al., 2009) as well as during an attentional task (Neuhaus et al., 2011; Uhlhaas et al., 2010).These results might point to a divergent mechanism, where the ACC and DLPFC seem to respond mostly by a hypoactivity in schizophrenia and by hyperactivity in 22q11.2DS, although as seen in Foxe et al. (2005) certain task conditions also lead to increased inferior frontal activations in schizophrenia.

Previously, in a study on auditory perception, an increased activity of anterior cingulate and medio-dorsal frontal cortex in 22q11.2DS was also found in the auditory modality (Rihs et al., 2013). Moreover, in task-negative conditions during rest, an increased duration and frequency was also observed for the EEG resting state that relates to dorsal ACC and insula activity and the salience network (Tomescu et al., 2014). This increase in activity was found both in 22q11.2DS and schizophrenia (Tomescu et al., 2015).

The salience network is thought to play an important role in recruiting relevant brain regions for processing of sensory information (Kapur, 2003; Menon, 2011) and the different activation of this network might point to aberrant salience processing that is present during rest but also during task conditions. It is possible that this aberrant activation could also impair the activation of sensory cortices as seen here for the visual modality and previously for auditory processing (Rihs et al., 2013).

In this study, we observe that both filling in and perceptual integration seem to be preserved in the 22q11.2DS group despite the early reduction in activity during the P1 and N1. The increased frontal activity could thus also reflect an increased effort to recruit sensory areas to achieve a comparable performance to controls. Increased activity of the ACC was also found during a visual go-no go task for the no-go condition in 22q11.2DS which could also point to increased compensatory activations (Romanos et al., 2010).

The following limitations of this study need to be considered. The sample is small and the age range is relatively large. We cannot exclude that the developmental changes of cortical thickness observed in 22q11.2DS might affect our results, given that frontal regions show a marked increase in cortical thickness during adolescence in 22q11.2DS (Schaer et al., 2009). While visual spatial contour integration and illusory contour perception is thought to have matured at the age of 14 years in the normal population (Kovács et al., 1999; Kovács, 2000; Nayar et al., 2015), we cannot exclude that delays in cortical maturation in 22q11.2DS might also have led to developmental delays in illusory contour perception affecting the younger participants in our cohort.

In summary, this study indicates deficits at early perceptual stages during the P1 and the N1, related to both ventral and dorsal visual processing. The reduction in amplitude and activity over visual areas are comparable to those observed in schizophrenia during the P1 component but continue during the N1 which appears less affected in people living with schizophrenia.

While an increase in amplitude during the Ncl inversely correlated with positive symptoms, the activations over LOC in the source space are comparable to the control group. Thus, consistent with findings in the schizophrenia literature, illusory contour perception seems to be preserved in 22q11.2DS despite the early visual deficits of the P1 and N1. The increased ACC and frontal lobe activation could reflect compensatory strategies used by 22q11.2DS participants to ensure higher performance and activation of lateral occipital cortex at later, conceptual stages of processing.

Acknowledgements

The authors would like to thank all the participants and their families who kindly volunteered to participate in this study. We extend our gratitude to Mathilde Bostelmann, Léa Chambaz, Lydia Dubourg, Johanna Maeder, Sarah Menghetti, Virginie Pouillard, Alexandra Zaharia, and Reem K. Jan, for trial coordination, clinical assessments and their help with data collection.

This study was supported by the National Centre of Competence in Research (NCCR) “SYNAPSY–The Synaptic Basis of Mental Diseases” (NCCR Synapsy Grant # “51NF40-158776”) and by the Swiss National Science Foundation (Grant Numbers: 320030_169206 to M.M.M.; 320030_159705 (current) and 324730-121996 (former) to C.M.M.; FNS 324730_144260 (current) to S.E.).

References

Akhtar, N., Enns, J.T., 1989. Relations between covert orienting and filtering in the development of visual attention. J. Exp. Child Psychol. 48, 315–334. http://dx.doi.org/10.1016/0022-0965(89)90008-8.

Allison, T., Puce, A., Spencer, D.D., McCarthy, G., 1999. Electrophysiological studies of human face perception. I: potentials generated in occipitotemporal cortex by face and non-face stimuli. Cereb. Cortex 9, 415–430. http://dx.doi.org/10.1093/cercor/9.5.415.

Antshel, K.M., Fremont, W., Kates, W.R., 2008. The neurocognitive phenotype in velocardio-facial syndrome: a developmental perspective. Dev. Disabil. Res. Rev. 14 (1), 43–51. http://dx.doi.org/10.1002/ddrr.7.

Bach, M., 2007. The Freiburg Visual Acuity Test-variability unchanged by post-hoc reanalysis. Graefes Arch. Clin. Exp. Ophthalmol. 245, 965–971. http://dx.doi.org/10.1007/s00417-006-0474-4.

Bearden, C.E., Woodin, M.F., Wang, P.P., Moss, E., McDonald-McGinn, D., Zackai, E., Cannon, T.D., 2001. The neurocognitive phenotype of the 22Q11.2 deletion syndrome: selective deficit in visual-spatial memory. J. Clin. Exp. Neuropsychol. 23 (4), 447–464. http://dx.doi.org/10.1076/jcen.23.4.447.1228.

Bostelmann, M., Schneider, M., Padula, M.C., Maeder, J., Schaer, M., Scariati, E., Debbané, M., Glaser, B., Menghetti, S., Eliez, S., 2016. Visual memory profile in 22q11.2 microdeletion syndrome: are there differences in performance and neurobiological substrates between tasks linked to ventral and dorsal visual brain structures? A cross-sectional and longitudinal study. J. Neurodev. Disord. 8, 41. http://dx.doi.org/10.1186/s11689-016-9174-5.

Brunet, D., Murray, M.M., Michel, C.M., 2011. Spatiotemporal analysis of multichannel EEG: CARTOOL. Comput. Intell. Neurosci. 2011. http://dx.doi.org/10.1155/2011/813870.

Butler, P.D., Schechter, I., Zemon, V., Schwartz, S.G., Greenstein, V.C., Gordon, J., Schroeder, C.E., Javitt, D.C., 2001. Dysfunction of early-stage visual processing in schizophrenia. Am. J. Psychiatry 158, 1126–1133. http://dx.doi.org/10.1176/appi.ajp.158.7.1126.

Butler, P.D., Abeles, I.Y., Silverstein, S.M., Dias, E.C., Weiskopf, N.G., Calderone, D.J., Sehatpour, P., 2013. An event-related potential examination of contour integration deficits in schizophrenia. Front. Psychol. 4, 1–12. http://dx.doi.org/10.3389/fpsyg.2013.00132.

Carey, A.H., Kelly, D., Halford, S., Wadey, R., Wilson, D., Goodship, J., Burn, J., Paul, T., Sharkey, A., Dumanski, J., Nordenskjold, M., Williamson, R., Scambler, P.J., 1992. Molecular genetic study of the frequency of monosomy 22q11 in DiGeorge syndrome. Am. J. Hum. Genet. 51, 964–970.

Christie, J., Klein, R., 1995. Familiarity and attention: does what we know affect what we notice? Mem. Cogn. 23, 547–550. http://dx.doi.org/10.3758/BF03197256.

Coon, H., Jensen, S., Holik, J., Hoff, M., Myles-Worsley, M., Reimherr, F., Wender, P., Waldo, M., Freedman, R., Leppert, M., Byerley, W., 1994. Genomic scan for genes predisposing to schizophrenia. Am. J. Med. Genet. 54, 59–71. http://dx.doi.org/10.1002/ajmg.1320540111.

Custo, A., Vulliemoz, S., Grouiller, F., Van De Ville, D., Michel, C., 2014. EEG source imaging of brain states using spatiotemporal regression. NeuroImage 96, 106–116. http://dx.doi.org/10.1016/j.neuroimage.2014.04.002.

Debbané, M., Glaser, B., Gex-Fabry, M., Eliez, S., 2005. Temporal perception in velocardio-facial syndrome. Neuropsychologia 43, 1754–1762. http://dx.doi.org/10.1016/j.neuropsychologia.2005.02.006.

Debbané, M., Glaser, B., David, M.K., Feinstein, C., Eliez, S., 2006. Psychotic symptoms in children and adolescents with 22q11.2 deletion syndrome: neuropsychological and behavioral implications. Schizophr. Res. 84, 187–193. http://dx.doi.org/10.1016/j.schres.2006.01.019.

Di Russo, F., Martínez, A., Sereno, M.I., Pitzalis, S., Hillyard, S.A., 2002. Cortical sources of the early components of the visual evoked potential. Hum. Brain Mapp. 15, 95–111. http://dx.doi.org/10.1002/hbm.10010.

Dias, E.C., Butler, P.D., Hoptman, M.J., Javitt, D.C., 2011. Early sensory contributions to contextual encoding deficits in schizophrenia. Arch. Gen. Psychiatry 68, 654. http://dx.doi.org/10.1001/archgenpsychiatry.2011.17.

Doniger, G.M., Foxe, J.J., Murray, M.M., Higgins, B.A., Snodgrass, J.G., Schroeder, C.E., Javitt, D.C., 2000. Activation timecourse of ventral visual stream object-recognition areas: high density electrical mapping of perceptual closure processes. J. Cogn. Neurosci. 12, 615–621. http://dx.doi.org/10.1162/089892900562372.

Doniger, G.M., Foxe, J.J., Schroeder, C.E., Murray, M.M., Higgins, B.A., Javitt, D.C., 2001. Visual perceptual learning in human object recognition areas: a repetition priming study using high-density electrical mapping. NeuroImage 13, 305–313. http://dx.doi.org/10.1006/nimg.2000.0684.

Doniger, G.M., Foxe, J.J., Murray, M.M., Higgins, B.A., Javitt, D.C., 2002. Impaired visual object recognition and dorsal/ventral stream interaction in schizophrenia. Arch. Gen. Psychiatry 59, 1011. http://dx.doi.org/10.1001/archpsyc.59.11.1011.

Emanuel, B.S., 2008. Molecular mechanisms and diagnosis of chromosome 22q11.2 rearrangements. Dev. Disabil. Res. Rev. 14, 11–18. http://dx.doi.org/10.1002/ddrr.3.

Fioravanti, M., Carlone, O., Vitale, B., Cinti, M.E., Clare, L., 2005. A meta-analysis of cognitive deficits in adults with a diagnosis of schizophrenia. Neuropsychol. Rev. 15, 73–95. http://dx.doi.org/10.1007/s11065-005-6254-9.

First, M.B., Spitzer, R.L., Gibbon, M., Williams, J.B.W, 1996. Structured Clinical Interview for DSM-IV Axis I Disorders, Clinician Version (SCID-CV). American Psychiatric Press, Inc., Washington, D.C.

Fisher, M., Loewy, R., Hardy, K., Schlosser, D., Vinogradov, S., 2013. Cognitive interventions targeting brain plasticity in the prodromal and early phases of schizophrenia. Annu. Rev. Clin. Psychol. 9, 435–463. http://dx.doi.org/10.1146/annurev-clinpsy-032511-143134.

Foxe, J.J., Doniger, G.M., Javitt, D.C., 2001. Early visual processing deficits in schizophrenia: impaired P1 generation revealed by high-density electrical mapping. Neuroreport 12, 3815–3820.

Foxe, J.J., Murray, M.M., Javitt, D.C., 2005. Filling-in in schizophrenia: a high-density electrical mapping and source-analysis investigation of illusory contour processing. Cereb. Cortex 15, 1914–1927. http://dx.doi.org/10.1093/cercor/bhi069.

Giersch, A., Glaser, B., Pasca, C., Chabloz, M., Debbané, M., Eliez, S., 2014. Individuals with 22q11.2 deletion syndrome are impaired at explicit, but not implicit, discrimination of local forms embedded in global structures. Am. J. Intellect. Dev. Disabil. 119, 261–275. http://dx.doi.org/10.1352/1944-7558-119.3.261.

Gourzis, P., Katrivanou, A., Beratis, S., 2002. Symptomatology of the initial prodromal phase in schizophrenia. Schizophr. Bull. 28, 415–429. http://dx.doi.org/10.1093/oxfordjournals.schbul.a006950.

Grave De Peralta Menendez, R., Murray, M.M., Michel, C.M., Martuzzi, R., Gonzalez Andino, S.L., 2004. Electrical neuroimaging based on biophysical constraints. NeuroImage 21, 527–539. http://dx.doi.org/10.1016/j.neuroimage.2003.09.051.

Grill-Spector, K., Kourtzi, Z., Kanwisher, N., 2001. The lateral occipital complex and its role in object recognition. Vis. Res. 41, 1409–1422. http://dx.doi.org/10.1016/S0042-6989(01)00073-6.

Hacıhamdioğlu, B., Hacıhamdioğlu, D., Delil, K., 2015. 22Q11 deletion syndrome: current perspective. Appl. Clin. Genet. 8, 123–132. http://dx.doi.org/10.2147/TACG.S82105.

Javitt, D.C., 2009. Sensory processing in schizophrenia: neither simple nor intact. Schizophr. Bull. 35, 1059–1064. http://dx.doi.org/10.1093/schbul/sbp110.

Javitt, D.C., Sweet, R.A., 2015. Auditory dysfunction in schizophrenia: integrating clinical and basic features. Nat. Rev. Neurosci. 16, 535–550. http://dx.doi.org/10.1038/nrn4002.

Johnson, S.C., Lowery, N., Kohler, C., Turetsky, B.I., 2005. Global–local visual processing in schizophrenia: evidence for an early visual processing deficit. Biol. Psychiatry 58, 937–946. http://dx.doi.org/10.1016/j.biopsych.2005.04.053.

Kanizsa, G., 1976. Subjective Contours. Sci. Am. 234, 48–52.

Kapur, S., 2003. Psychosis as a state of aberrant salience: a framework linking biology, phenomenology, and pharmacology in schizophrenia. Am. J. Psychiatry 160, 13–23. http://dx.doi.org/10.1176/appi.ajp.160.1.13.

Karayiorgou, M., Simon, T.J., Gogos, J.A., 2010. 22q11.2 microdeletions: linking DNA structural variation to brain dysfunction and schizophrenia. Nat. Rev. Neurosci. 11, 402–416. http://dx.doi.org/10.1038/nrn2841.

Kates, W.R., Antshel, K.M., Faraone, S.V., Fremont, W.P., Marie, A., Shprintzen, R.J., Botti, J., Kelchner, L., McCarthy, C., 2012. Neuroanatomic predictors to prodromal psychosis in velocardiofacial syndrome (22q11.2 deletion syndrome): a longitudinal study. J. Biol. Psychiatry 69, 945–952. http://dx.doi.org/10.1016/j.biopsych.2010.10.027.

Kay, S.R., Fiszbein, A., Opler, L.A., 1987. The positive and negative syndrome scale (PANSS) for schizophrenia. Schizophr. Bull. 13 (2), 261–276.

Keane, B.P., Joseph, J., Silverstein, S.M., 2014. Late, not early, stages of Kanizsa shape perception are compromised in schizophrenia. Neuropsychologia 56, 302–311. http://dx.doi.org/10.1016/j.neuropsychologia.2014.02.001.

Knebel, J.F., Javitt, D.C., Murray, M.M., 2011. Impaired early visual response modulations to spatial information in chronic schizophrenia. Psychiatry Res. Neuroimaging 193, 168–176. http://dx.doi.org/10.1016/j.pscychresns.2011.02.006.

Koenig, Thomas, Melie-Garcia, Lester, 2010. A method to determine the presence of averaged event-related fields using randomization tests. Brain Topogr. 23, 233–242. http://dx.doi.org/10.1007/s10548-010-0142-1.

Kovács, I., 2000. Human development of perceptual organization. Vis. Res. 40 (10), 1301–1310.

Kovács, I., Kozma, P., Fehér, Á., Benedek, G., 1999. Late maturation of visual spatial integration in humans. Proc. Natl. Acad. Sci. 96 (2l), 12204–12209.

Lehmann, D., Skrandies, W., 1980. Reference-free identification of components of checkerboard-evoked multichannel potential fields. Electroencephalogr. Clin. Neurophysiol. 48, 609–621. http://dx.doi.org/10.1016/0013-4694(80)90419-8.

Lesher, G.W., 1995. Illusory contours: toward a neurally based perceptual theory. Psychon. Bull. Rev. 2 (3), 279–321. http://dx.doi.org/10.3758/BF03210970.

Luck, S.J., Mathalon, D.H., Donnell, B.F.O., Hämäläinen, M.S., Spencer, K.M., 2011. A roadmap for the development and validation of ERP biomarkers in schizophrenia research. Biol. Psychiatry 70, 28–34. http://dx.doi.org/10.1016/j.biopsych.2010.09.021.A.

McGlashan, T.H., Johannessen, J.O., 1996. Early detection and intervention with schizophrenia: rationale. Schizophr. Bull. 22, 201–222. http://dx.doi.org/10.1093/schbul/22.2.201.

McGlashan, T.H., Miller, T.J., Woods, S.W., Hoffman, R.E., Davidson, L., 2001. Instrument for the assessment of prodromal symptoms and states. In: Early Intervention in Psychotic Disorders. Springer Netherlands, Dordrecht, pp. 135–149. http://dx.doi.org/10.1007/978-94-010-0892-1_7.

Menon, V., 2011. Large-scale brain networks and psychopathology: a unifying triple network model. Trends Cogn. Sci. 15, 483–506. http://dx.doi.org/10.1016/j.tics.2011.08.003.

Michel, C.M., Murray, M.M., 2011. Towards the utilization of EEG as a brain imaging tool. NeuroImage 61, 371–385. http://dx.doi.org/10.1016/j.neuroimage.2011.12.039.

Michel, C.M., Thut, G., Morand, S., Khateb, A., Pegna, A.J., Grave de Peralta, R., Gonzales, S., Seeck, M., Landis, T., 2001. Electric source imaging of human cognitive brain functions. A review. Brain Res. Rev. 36, 108–118. http://dx.doi.org/10.1016/S0165-0173(01)00086-8.

Miller, T.J., McGlashan, T.H., Woods, S.W., Stein, K., Driesen, N., Corcoran, C.M., Hoffman, R., Davidson, L., 1999. Symptom assessment in schizophrenic prodromal states. Psychiatr. Q. 70, 273–287. http://dx.doi.org/10.1023/a:1022034115078.

Miller, T.J., McGlashan, T.H., Rosen, J.L., Cadenhead, K., Ventura, J., Mcfarlane, W., Perkins, D.O., Pearlson, Q.D., Woods, S.W., 2003. Prodromal assessment with the structured interview for prodromal syndromes and the scale of prodromal symptoms: predictive validity, interrater reliability, and training to reliability. Schizophr. Bull. 29, 703–715. http://dx.doi.org/10.1093/oxfordjournals.schbul.a007040.

Morrison, A.P., French, P., Parker, S., Roberts, M., Stevens, H., Bentall, R.P., Lewis, S.W., 2007. Three-year follow-up of a randomized controlled trial of cognitive therapy for the prevention of psychosis in people at ultrahigh risk. Schizophr. Bull. 33, 682–687. http://dx.doi.org/10.1093/schbul/sbl042.

Murray, M.M., Herrmann, C.S., 2013. Illusory contours: a window onto the neurophysiology of constructing perception. Trends Cogn. Sci. 17, 471–481. http://dx.doi.org/

10.1016/j.tics.2013.07.004.
Murray, M.M., Foxe, J.J., Higgins, B.A., Javitt, D.C., Schroeder, C.E., 2001. Visuo-spatial neural response interactions in early cortical processing during a simple reaction time task: a high-density electrical mapping study. Neuropsychologia 39 (8), 828–844. http://dx.doi.org/10.1016/S0028-3932(01)00004-5.
Murray, M.M., Wylie, G.R., Higgins, B.A., Javitt, D.C., Schroeder, C.E., Foxe, J.J., 2002. The spatiotemporal dynamics of illusory contour processing: combined high-density electrical mapping, source analysis, and functional magnetic resonance imaging. J. Neurosci. 22 (12), 5055–5073.
Murray, M.M., Imber, M.L., Javitt, D.C., Foxe, J.J., 2006. Boundary completion is automatic and dissociable from shape discrimination. J. Neurosci. 26 (46), 12043–12054. http://dx.doi.org/10.1523/JNEUROSCI.3225-06.2006.
Murray, M.M., Brunet, D., Michel, C.M., 2008. Topographic ERP analyses: a step-by-step tutorial review. Brain Topogr. 20, 249–264. http://dx.doi.org/10.1007/s10548-008-0054-5.
Nayar, K., Franchak, J., Adolph, K., Kiorpes, L., 2015. From local to global processing: the development of illusory contour perception. J. Exp. Child Psychol. 131, 38–55. http://dx.doi.org/10.1016/j.jecp.2014.11.001.
Neuhaus, A.H., Karl, C., Hahn, E., Trempler, N.R., Opgen-Rhein, C., Urbanek, C., Hahn, C., Ta, T.M., Dettling, M., 2011. Dissection of early bottom-up and top-down deficits during visual attention in schizophrenia. Clin. Neurophysiol. 122, 90–98. http://dx.doi.org/10.1016/j.clinph.2010.06.011.
Notredame, C.-E., Pins, D., Deneve, S., Jardri, R., 2014. What visual illusions teach us about schizophrenia. Front. Integr. Neurosci. 8, 63. http://dx.doi.org/10.3389/fnint.2014.00063.
Oribe, N., Hirano, Y., Kanba, S., del Re, E.C., Seidman, L.J., Mesholam-Gately, R., Spencer, K.M., McCarley, R.W., Niznikiewicz, M.A., 2013. Early and late stages of visual processing in individuals in prodromal state and first episode schizophrenia: an ERP study. Schizophr. Res. 146, 95–102. http://dx.doi.org/10.1016/j.schres.2013.01.015.
Óskarsdóttir, S., Persson, C., Eriksson, B.O., Fasth, A., 2005. Presenting phenotype in 100 children with the 22q11 deletion syndrome. Eur. J. Pediatr. 164, 146–153. http://dx.doi.org/10.1007/s00431-004-1577-8.
Perrin, F., Pernier, J., Bertrand, O., Echallier, J.F., 1989. Spherical splines for scalp potential and current density mapping. Electroencephalogr. Clin. Neurophysiol. 72, 184–187. http://dx.doi.org/10.1016/0013-4694(89)90180-6.
Plomp, G., Roinishvili, M., Chkonia, E., Kapanadze, G., Kereselidze, M., Brand, A., Herzog, M.H., 2013. Electrophysiological evidence for ventral stream deficits in schizophrenia patients. Schizophr. Bull. 39, 547–554. http://dx.doi.org/10.1093/schbul/sbr175.
R Core Team, 2013. R: A language and environment for statistical computing. R Foundation for Statistical Computing, Vienna, Austria. http://www.R-project.org.
Reich, W., 2000. Diagnostic Interview for Children and Adolescents (DICA). J. Am. Acad. Child Adolesc. Psychiatry 39, 59–66. http://dx.doi.org/10.1097/00004583-200001000-00017.
Rihs, T.A., Tomescu, M.I., Britz, J., Rochas, V., Custo, A., Schneider, M., Debbané, M., Eliez, S., Michel, C.M., 2013. Altered auditory processing in frontal and left temporal cortex in 22q11.2 deletion syndrome: a group at high genetic risk for schizophrenia. Psychiatry Res. Neuroimaging 212, 141–149. http://dx.doi.org/10.1016/j.pscychresns.2012.09.002.
Romanos, M., Ehlis, A.C., Baehne, C.G., Jacob, C., Renner, T.J., Storch, A., Briegel, W., Walitza, S., Lesch, K.P., Fallgatter, A.J., 2010. Reduced NoGo-anteriorisation during continuous performance test in deletion syndrome 22q11.2. J. Psychiatr. Res. 44, 768–774. http://dx.doi.org/10.1016/j.jpsychires.2010.02.001.
Scambler, P.J., 2000. The 22q11 deletion syndromes. Hum. Mol. Genet. Rev. 9, 2421–2426.
Scariati, E., Schaer, M., Richiardi, J., Schneider, M., Debbané, M., Van De Ville, D., Eliez, S., 2014. Identifying 22q11.2 deletion syndrome and psychosis using resting-state connectivity patterns. Brain Topogr. 27 (6), 808–821. http://dx.doi.org/10.1007/s10548-014-0356-8.
Schaer, M., Debbané, M., Bach Cuadra, M., Ottet, M.C., Glaser, B., Thiran, J.P., Eliez, S., 2009. Deviant trajectories of cortical maturation in 22q11.2 deletion syndrome (22q11DS): a cross-sectional and longitudinal study. Schizophr. Res. 115, 182–190. http://dx.doi.org/10.1016/j.schres.2009.09.016.
Schaer, M., Glaser, B., Ottet, M.-C., Schneider, M., Meritxell, Cuadra, B., Debbané, M., Thiran, J.-P., Eliez, S., Schaer, M., Glaser, B., Ottet, M.-C., Schneider, M., Debbané, M., Eliez, S., Ottet, M.-C., Schneider, M., Debbané, M., Bach Cuadra, M., Thiran, J.-P., 2010. Regional cortical volumes and congenital heart disease: a MRI study in 22q11.2 deletion syndrome. J. Neurodev. Disord. 2, 224–234. http://dx.doi.org/10.1007/s11689-010-9061-4.
Schneider, W., Eschman, A., Zuccolotto, A., 2002. E-Prime User's Guide. Psychology Software Tools Inc., Pittsburgh (version).
Schneider, M., van der Linden, M., Glaser, B., Debbané, M., Eliez, S., 2011. Evolution and predictive value of attenuated negative symptoms in 22qDS. Int. Clin. Psychopharmacol. 26, e142. http://dx.doi.org/10.1097/01.yic.0000405874.79590.16.
Schneider, M., Schaer, M., Mutlu, A.K., Menghetti, S., Glaser, B., Debbané, M., Eliez, S., 2014a. Clinical and cognitive risk factors for psychotic symptoms in 22q11.2 deletion syndrome: a transversal and longitudinal approach. Eur. Child Adolesc. Psychiatry 23, 425–436. http://dx.doi.org/10.1007/s00787-013-0469-8.
Schneider, M., Van der Linden, M., Menghetti, S., Glaser, B., Debbané, M., Eliez, S., 2014b. Predominant negative symptoms in 22q11.2 deletion syndrome and their associations with cognitive functioning and functional outcome. J. Psychiatr. Res. 48, 86–93. http://dx.doi.org/10.1016/j.jpsychires.2013.10.010.
Sehatpour, P., Dias, E.C., Butler, P.D., Revheim, N., Guilfoyle, D.N., Foxe, J.J., Javitt, D.C., Javitt, D., Jalbrzikowski, M., Javitt, D., Rosen, B., Halgren, E., Keefe, R., Kraemer, H., Mesholam-Gately, R., Seidman, L., Stover, E., Weinberger, D., Young, A., Zalcman, S., Marder, S., 2010. Impaired visual object processing across an occipital-frontal-hippocampal brain network in schizophrenia. Arch. Gen. Psychiatry 67 (8), 772–782. http://dx.doi.org/10.1001/archgenpsychiatry.2010.85.
Senkowski, D., Röttger, S., Grimm, S., Foxe, J.J., Herrmann, C.S., 2005. Kanizsa subjective figures capture visual spatial attention: evidence from electrophysiological and behavioral data. Neuropsychologia 43 (6), 872–886. http://dx.doi.org/10.1016/j.neuropsychologia.2004.09.010.
Shapiro, H.M., Takarae, Y., Harvey, D.J., Cabaral, M.H., Simon, T.J., 2012. A cross-sectional study of the development of volitional control of spatial attention in children with chromosome 22q11.2 deletion syndrome. J. Neurodev. Disord. 4 (1), 5. http://dx.doi.org/10.1186/1866-1955-4-5.
Shpaner, M., Molholm, S., Forde, E., Foxe, J.J., 2013. Disambiguating the roles of area V1 and the lateral occipital complex (LOC) in contour integration. NeuroImage 69, 146–156. http://dx.doi.org/10.1016/j.neuroimage.2012.11.023.
Shprintzen, R.J., 2008. Velo-cardio-facial syndrome: 30 years of study. Dev. Disabil. Res. Rev. 14, 3–10. http://dx.doi.org/10.1002/ddrr.2.
Silverstein, S.M., Keane, B.P., 2011. Perceptual organization impairment in schizophrenia and associated brain mechanisms: review of research from 2005 to 2010. Schizophr. Bull. 37, 690–699. http://dx.doi.org/10.1093/schbul/sbr052.
Silverstein, S.M., Berten, S., Essex, B., Kovács, I., Susmaras, T., Little, D.M., 2009. An fMRI examination of visual integration in schizophrenia. J. Integr. Neurosci. 8, 175–202. http://dx.doi.org/10.1167/9.8.904.
Simon, T.J., 2008. A new account of the neurocognitive foundations of impairments in space, time, and number processing in children with chromosome 22q11.2 deletion syndrome. Dev. Disabil. Res. Rev. 14 (1), 52–58. http://dx.doi.org/10.1002/ddrr.8.
Snodgrass, J.G., Feenan, K., 1990. Priming effects in picture fragment completion: support for the perceptual closure hypothesis. J. Exp. Psychol. Gen. 119, 276–296. http://dx.doi.org/10.1037/0096-3445.119.3.276.
Spinelli, L., Andino, S.G., Lantz, G., Seeck, M., Michel, C.M., 2000. Electromagnetic inverse solutions in anatomically constrained spherical head models. Brain Topogr. 13, 115–125. http://dx.doi.org/10.1023/A:1026607118642.
Tomescu, M.I., Rihs, T.A., Becker, R., Britz, J., Custo, A., Grouiller, F., Schneider, M., Debbané, M., Eliez, S., Michel, C.M., 2014. Deviant dynamics of EEG resting state pattern in 22q11.2 deletion syndrome adolescents: a vulnerability marker of schizophrenia? Schizophr. Res. 157, 175–181. http://dx.doi.org/10.1016/j.schres.2014.05.036.
Tomescu, M.I., Rihs, T.A., Roinishvili, M., Karahanoglu, F.I., Schneider, M., Menghetti, S., Van De Ville, D., Brand, A., Chkonia, E., Eliez, S., Herzog, M.H., Michel, C.M., Cappe, C., 2015. Schizophrenia patients and 22q11.2 deletion syndrome adolescents at risk express the same deviant patterns of resting state EEG microstates: a candidate endophenotype of schizophrenia. Schizophr. Res. Cogn. 2, 159–165. http://dx.doi.org/10.1016/j.scog.2015.04.005.
Uhlhaas, P.J., Silverstein, S.M., 2005. Perceptual organization in schizophrenia spectrum disorders: empirical research and theoretical implications. Psychol. Bull. 131, 618–632. http://dx.doi.org/10.1037/0033-2909.131.4.618.
Uhlhaas, P.J., Phillips, W.A., Mitchell, G., Silverstein, S.M., 2006. Perceptual grouping in disorganized schizophrenia. Psychiatry Res. 145, 105–117. http://dx.doi.org/10.1016/j.psychres.2005.10.016.
Uhlhaas, P.J., Roux, F., Rodriguez, E., Rotarska-Jagiela, A., Singer, W., 2010. Neural synchrony and the development of cortical networks. Trends Cogn. Sci. 14, 72–80. http://dx.doi.org/10.1016/j.tics.2009.12.002.
Woldorff, M.G., Fox, P.T., Matzke, M., Lancaster, J.L., Veeraswamy, S., Zamarripa, F., Seabolt, M., Glass, T., Gao, J.H., Martin, C.C., Jerabek, P., 1997. Retinotopic organization of early visual spatial attention effects as revealed by PET and ERPs. Hum. Brain Mapp. 5, 280–286. http://dx.doi.org/10.1002/(SICI)1097-0193(1997)5:4<280::AID-HBM13>3.0.CO;2-I.
Yamagishi, H., 2002. The 22q11.2 deletion syndrome. Keio J. Med. 51 (2), 77–88.
Yeap, S., Kelly, S.P., Sehatpour, P., Magno, E., Javitt, D.C., Garavan, H., Thakore, J.H., Foxe, J.J., 2006. Early visual sensory deficits as endophenotypes for schizophrenia. Arch. Gen. Psychiatry 63, 1180. http://dx.doi.org/10.1001/archpsyc.63.11.1180.